S1. List of the primary antibodies used and their optimised immunohistochemistry protocol.

Target	Primary Antibody	Antibody dilution	Clone	Antigen Retrieval	Incubation Settings
PLP	Biorad #MCA839G	1 : 1000	monoclonal	Citrate pH6 microwave	1h RT
CD68	Dako #M0874	1 : 50	monoclonal	Citrate pH6 Autoclave	1h RT
CD3	Dako #A0452	1 : 100	polyclonal	Tris-EDTA pH 9 Autoclave	1h RT
CD20	Dako #IS604	Ready to use	monoclonal	Citrate pH6 microwave	1h RT
C9neo	Hycult Biotech #HM2264	1:100	monoclonal	Tris-EDTA pH 9 Autoclave	1h RT
βAPP	Millipore#MAB348	1:5000	monoclonal	Citrate pH6 Autoclave followed by 5 minutes Formic acid	1h RT
GFAP	Dako #Z0334	1 : 4000	polyclonal	Citrate pH6 microwave	1h RT
AQP4	Millipore #AB3594	1 : 750	polyclonal	Citrate pH6 autoclave	1h RT

S2. Characteristics of the inflammatory infiltrate in the anterior optic pathway demyelinating lesions.

Multiple sclerosis

In the multiple sclerosis cohort, the majority of multiple sclerosis cases showed evidence of inflammatory activity (i.e. active and mixed active/inactive) as it was found in 34 (73.9%) samples from 24 cases (75%). In particular, 4 donors presented acute active plaques (16.7% of donors - 6 samples), 8 had mixed active-inactive lesions (33.3% of donors - 9 samples), 6 presented both chronic inactive and mixed active-inactive lesions (25% of donors - 19 samples). The remaining 6 donors had chronic inactive plaques only (25% of donors - 12 samples).

The inflammatory features of the lesion types we identified in the anterior optic pathway resemble those usually observed in the rest of the CNS. Chronic inactive plaques displayed a mild and diffuse inflammatory activity. Some CD68+ microglia and CD3+ lymphocytes widespread throughout the plaque area, the lesion border and the surrounding myelinated white matter, without significant differences between these areas. The number of inflammatory cells detected in each area was slightly higher than observed in non-neurological controls ($p<0.05$ considering the semi quantitative scores of CD68+ and CD3+ elements in the parenchyma and in the perivascular area of plaque and peri-plaque; $p<0.05$ for CD68+ elements in the parenchyma and in the perivascular area of surrounding non-lesional white matter; see table and figure below) and, as expected, much lower than observed in active or mixed active-inactive MS lesions.

Mixed active-inactive plaques presented a typical border active pattern with a relatively inactive lesion core. The classic feature of a rim of microglia CD68+ at the edge of the plaque was not clearly visible in our samples, as found in other areas of the CNS. This was possibly due to the denser packaging of nerve bundles in the anterior optic pathway preventing the organization of the inflammatory border. Nevertheless, the border area had more inflammatory activity compared with both the plaque area ($p\leq0.05$ considering CD68+ pixel count and the semiquantitative scores of CD68+ and CD3+ elements in the parenchyma and in the perivascular area) and the surrounding non-lesional white matter ($p\leq0.05$ considering the semi quantitative scores of CD68+ elements in the parenchyma and in the perivascular area). Even in the inactive lesion core, inflammatory elements were more frequent than in control donors ($p<0.05$ considering CD68+ pixel count and the semiquantitative scores of CD68+ and CD3+ elements in the parenchyma and in the perivascular area) or in chronic inactive MS plaques ($p<0.05$ considering CD68+ pixel count and the

semiquantitative scores of parenchymal and vascular CD68+ elements, while CD3+ cells did not significantly differ). Therefore, inflammatory activity in mixed active-inactive plaques was predominant but not exclusively found at the plaque edge (see table and figure below).

Finally, acute active lesions were more densely inflamed than inactive or mixed active-inactive lesions ($p<0.005$ considering CD68+ pixel count and the semiquantitative scores of CD68+ and CD3+ elements in the parenchyma and in the perivascular area), and display a diffuse and homogeneous infiltration, without significant differences between the plaque area, the lesion border and the adjacent myelinated area - except for a lower inflammatory activity in the surrounding non-lesional white matter compared with the border of the lesions when considering parenchymal CD68+ and CD3+ elements ($p=0.008$ and $p<0.001$, respectively). In acute active lesions, sparse CD68+ elements presented either microglial or macrophagic phenotype, the latter sometimes had PLP positive debris within the cytoplasm (see table and figure below).

Neuromyelitis optica spectrum disorder

In neuromyelitis optica spectrum disorder cases, the inflammation did not present significant differences compared with active MS cases, except for the fact that the border of the neuromyelitis optica spectrum disorder lesions tended to have less CD3 and CD68 infiltration compared with the lesion core, but not significantly so (see table and figure below).

Acute disseminated encephalomyelitis

In the acute disseminated encephalomyelitis cases, the small demyelinating area did not allow to semiquantitative score the inflammatory infiltrate in the plaque area with the same method used for multiple sclerosis and neuromyelitis optica spectrum disorder cases.

Table. *The table reports all the data regarding inflammatory infiltrates in demyelinating plaques of multiple sclerosis and neuromyelitis optica spectrum disorder cases; multiple sclerosis lesions are divided according to plaque type (chronic inactive, mixed active-inactive and acute active). Data derived from the anterior optic nerve pathway of non-neurological controls are reported as reference values. CD68 indicate microglial infiltration and has been measured using an automated positive pixel count protocol (positive pixel per micrometer), also semiquantitative assessment of CD3+ lymphocytes and CD68+ microglia in the parenchyma (ranging 0 to 3) and in the perivascular space (ranging 0 to 4) has been scored.*

	Plaque type	Area	Mean	Std. Error	95% Wald Confidence Interval	
					Lower	Upper
CD68 positive pixel count	Controls	NAWM	156,39	27,08	103,31	209,46
	MS - inactive	Plaque	201,71	73,27	58,11	345,32
		Peri-plaque	171,11	59,62	54,27	287,96
		NAWM	169,46	51,32	68,88	270,05
	MS - mixed active	Plaque	726,70	143,42	445,60	1.007,81
		Peri-plaque	4.411,32	1.234,63	1.991,48	6.831,15
		NAWM	3.710,51	1.136,42	1.483,17	5.937,84
	MS - active	Plaque	18.261,95	8.975,27	670,74	35.853,15
		Peri-plaque	12.556,04	3.417,09	5.858,68	19.253,40
		NAWM	8.779,00	0,00	8.779,00	8.779,00
	NMOSD	Plaque	29.059,39	9.707,81	10.032,42	48.086,35
		Peri-plaque	1.843,50	0,00	1.843,50	1.843,50
CD68 semiquantitative - parenchyma	Controls	NAWM	0,00	0,00	0,00	0,00
	MS - inactive	Plaque	0,13	0,05	0,05	0,22
		Peri-plaque	0,22	0,08	0,07	0,37
		NAWM	0,32	0,16	0,00	0,64
	MS - mixed active	Plaque	0,62	0,12	0,39	0,86
		Peri-plaque	1,81	0,11	1,59	2,03
		NAWM	1,45	0,21	1,04	1,85
	MS - active	Plaque	2,17	0,24	1,70	2,64
		Peri-plaque	2,66	0,20	2,26	3,06
		NAWM	2,13	0,00	2,13	2,13
	NMOSD	Plaque	1,63	0,26	1,13	2,13
		Peri-plaque	1,00	0,00	1,00	1,00
CD68 semiquantitative - vessels	Controls	NAWM	0,01	0,01	-0,01	0,02
	MS - inactive	Plaque	0,32	0,11	0,10	0,54
		Peri-plaque	0,25	0,08	0,09	0,42
		NAWM	0,33	0,09	0,15	0,50
	MS - mixed active	Plaque	0,90	0,17	0,57	1,23
		Peri-plaque	1,66	0,09	1,48	1,84
		NAWM	1,25	0,20	0,85	1,64
	MS - active	Plaque	2,35	0,27	1,81	2,89
		Peri-plaque	2,42	0,21	2,01	2,83
		NAWM	2,38	0,00	2,38	2,38
	NMOSD	Plaque	2,31	0,36	1,61	3,01
		Peri-plaque	1,50	0,00	1,50	1,50

	Plaque type	Area	Mean	Std. Error	95% Wald Confidence Interval	
					Lower	Upper
CD3 semiquantitative - parenchyma	Controls	NAWM	0,03	0,02	-0,01	0,07
	MS - inactive	Plaque	0,59	0,21	0,17	1,00
		Peri-plaque	0,32	0,17	-0,02	0,67
		NAWM	0,05	0,04	-0,03	0,13
	MS - mixed active	Plaque	0,79	0,25	0,30	1,29
		Peri-plaque	1,26	0,32	0,64	1,88
		NAWM	1,12	0,31	0,53	1,72
	MS - active	Plaque	2,61	0,23	2,15	3,07
		Peri-plaque	2,48	0,15	2,18	2,78
		NAWM	1,88	0,00	1,88	1,88
	NMOSD	Plaque	2,31	0,20	1,91	2,71
		Peri-plaque	3,00	0,00	3,00	3,00
CD3 semiquantitative - vessels	Controls	NAWM	0,30	0,12	0,07	0,54
	MS - inactive	Plaque	0,99	0,26	0,49	1,50
		Peri-plaque	1,15	0,25	0,67	1,64
		NAWM	0,55	0,19	0,17	0,92
	MS - mixed active	Plaque	1,16	0,21	0,75	1,56
		Peri-plaque	1,53	0,17	1,20	1,85
		NAWM	1,39	0,27	0,87	1,90
	MS - active	Plaque	2,85	0,22	2,43	3,27
		Peri-plaque	2,46	0,28	1,91	3,01
		NAWM	2,75	0,00	2,75	2,75
	NMOSD	Plaque	2,42	0,15	2,13	2,71
		Peri-plaque	2,50	0,00	2,50	2,50

Figure. *The boxplots display the features of inflammatory infiltrates in demyelinating plaques of multiple sclerosis lesions by comparing: chronic inactive, mixed active-inactive and acute active plaques. Data derived from the anterior optic nerve pathway of non-neurological controls are also reported as reference values. CD68 indicate microglial infiltration and has been measured using an automated positive pixel count protocol (positive pixel per micrometer), also semiquantitative assessment of CD3+ lymphocytes and CD68+ microglia in the parenchyma (ranging 0 to 3) and in the perivascular space (ranging 0 to 4) has been scored.*

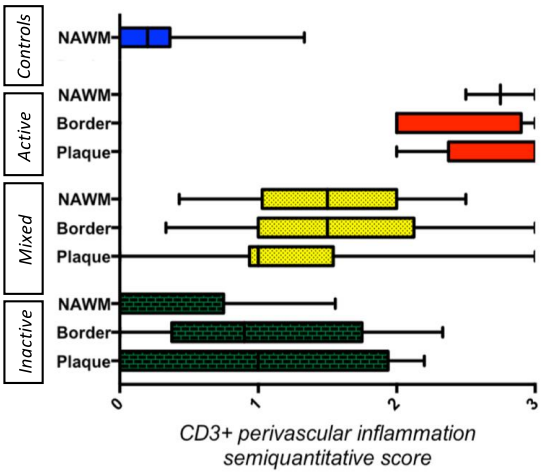
Controls
Active
Mixed
Inactive
NAWM
Border
Plaque
0
1
2
3
CD3+ perivascular inflammation
semiquantitative score

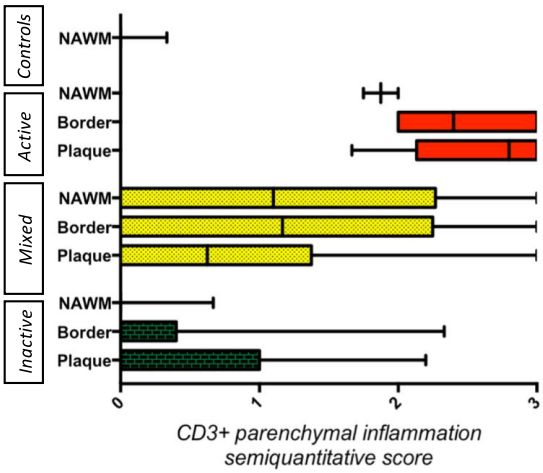
Controls
Active
Mixed
Inactive
NAWM
Border
Plaque
0
1
2
3
CD3+ parenchymal inflammation
semiquantitative score

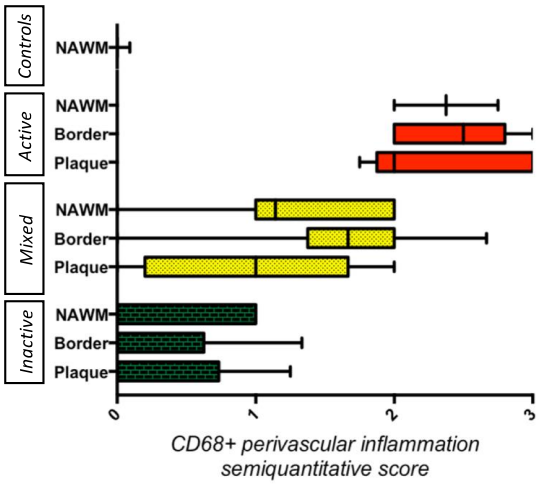
Controls
Active
Mixed
Inactive
NAWM
Border
Plaque
0
1
2
3
CD68+ perivascular inflammation
semiquantitative score

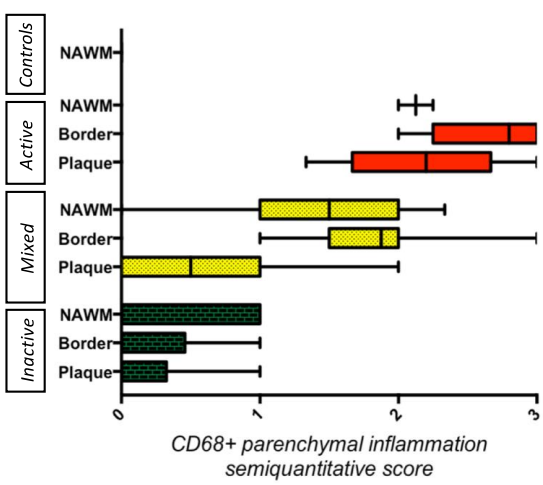
Controls
Active
Mixed
Inactive
NAWM
Border
Plaque
0
1
2
3
CD68+ parenchymal inflammation
semiquantitative score

Supplementary data, S3. Characterisitics of the non-lesional white matter

Multiple sclerosis

On evaluation of samples without evidence of demyelination (27 samples from 14 cases), diffuse CD68+ microglial/macrophage and CD3+ lymphocyte infiltration was observed in the parenchyma and in the perivascular space. Inflammation in the normal appearing white matter compartment was higher in multiple sclerosis cases compared to controls (*CD68*: perivascular score, Wald 7.87, p=0.005; parenchymal score, Wald 7.7, p=0.006; pixel count, Wald 4.82, p=0.028. *CD3*: perivascular score, Wald 12.5, p<0.001; parenchymal score, Wald 6.46, p=0.011). Sensitivity analysis considering only the multiple sclerosis cases without demyelinating lesions in the whole sampled area (5 donors, 7 samples) yielded similar findings. CD20+ B-cells were not found.

Cases older than 60 years tended to have higher inflammation in the normal appearing white matter compared with cases younger than 60 years (CD68 pixel count, 469 pixels/nm^2; CI95% 182 – 758 vs 2956 pixels/nm^2; CI95% 74 – 5837; Wald 2.83, p=0.093. CD3 perivascular score, 0.61; CI95% 0.22 – 1 vs 1.17; CI95% 0.92 – 1.42; Wald 5.5, p=0.019). Cases with disease duration longer than 20 years tended to show higher inflammation in the normal appearing white matter compared with cases with shorter duration disease (CD68 perivascular score, 0.489; CI95% 0.116 – 1.094 vs 1.765; CI95% 0.605 – 2.924; Wald 3.66, p=0.056).

Neuromyelitis optica spectrum disorder

On considering the neuromyelitis optica spectrum disorder cases without evidence of demyelination (4 cases, 18 samples), microglial/macrophage and T-cell inflammatory scores were higher than controls (CD68: perivascular score, Wald 12.17, p<0.001; parenchymal score, Wald 8.18, p=0.004; pixel count, Wald 4.54, p=0.033. CD3: perivascular score, Wald 8.33, p=0.004; parenchymal score, Wald 3.81, p=0.051). CD20+ B-cell lymphocytes were detected in the 33.3% of the samples (6/18 samples; 2/4 cases) (CD20: neuromyelitis optica spectrum disorder versus control: Chi-square 9.931, p=0.0016). Of note, none of the four neuromyelitis spectrum disorder cases without demyelination included in this analysis had a history of optic neuritis.

Acute disseminated encephalomyelitis

Normal appearing white matter (5 subjects, 10 samples) showed a predominant T-cell lymphocyte infiltration above that of controls (CD3: perivascular score, Wald 7.81, p=0.005; parenchymal score, Wald 4.56, p=0.033). However, the extent CD68+ microglial/macrophage infiltration in the

parenchyma or perivascular space did not differ from controls (p>0.1 in all the analyses). CD20+ B-cells were not found.

Comparisons between CNS demyelinating diseases

CD20+ B-cell lymphocytes were higher in neuromyelitis optica spectrum disorder cases compared to multiple sclerosis and acute disseminated encephalomyelitis cases (Chi-square 14, p=0.001). Acute disseminated encephalomyelitis cases demonstrated more extensive CD3+ lymphocyte perivascular infiltration than that observed in multiple sclerosis and neuromyelitis optica spectrum disorder cases (despite statistical significance was not reached in these analyses). CD68 inflammation tended to be lower in acute disseminated encephalomyelitis compared with multiple sclerosis (pixel count, Wald 3.7, p=0.055; parenchymal score, Wald 3.38, p=0.066) and neuromyelitis optica spectrum disorder cases (pixel count, Wald 3.55, p=0.059; parenchymal score, Wald 5.25, p=0.022).

Table. *The table reports all the data regarding inflammatory infiltrates in the non-lesional white matter of 5 controls, 5 ADEM, 14 MS and 4 NMOSD donors. Only samples without demyelination were considered. CD68 indicates microglial infiltration and has been measured using an automated positive pixel count protocol (positive pixel per micrometer). A semiquantitative assessment of CD3+ lymphocytes and CD68+ microglia in the parenchyma and in the perivascular space (ranging 0 to 3) is also reported.*

	Mean	Std. Error	95% Wald Confidence Interval	
			Lower	Upper
CD68 positive pixel count				
Controls	156,39	27,08	103,31	209,46
ADEM	364,98	151,13	68,78	661,19
MS	2034,85	855,29	358,51	3711,18
NMOSD	2162,08	941,39	316,98	4007,17
CD68 semiquantitative - parenchyma				
Controls	0,00	0,00	0,00	0,00
ADEM	0,19	0,13	-0,06	0,44
MS	0,72	0,26	0,21	1,24
NMOSD	1,18	0,41	0,37	1,99
CD68 semiquantitative - vessel				
Controls	0,01	0,01	-0,01	0,02
ADEM	0,65	0,41	-0,15	1,46
MS	0,77	0,27	0,24	1,31
NMOSD	1,06	0,30	0,47	1,65
CD3 semiquantitative - parenchyma				
Controls	0,03	0,02	-0,01	0,07
ADEM	1,23	0,56	0,13	2,33
MS	0,56	0,21	0,15	0,97
NMOSD	0,80	0,40	0,02	1,58
CD3 semiquantitative - vessel				
Controls	0,30	0,12	0,07	0,54
ADEM	1,69	0,50	0,71	2,68
MS	0,96	0,14	0,68	1,24
NMOSD	1,29	0,32	0,66	1,93

S4. GFAP and AQP4 expression.

Because of the vascular anatomy, both GFAP and AQP4 featured an intense rosette-like staining in sagittal sections while a linear, stripe-like and dotted staining was found in longitudinal sections.
For this reason, the sagittal sections showed a higher GFAP pixel intensity (0.129 pixels/um^2; CI95% 0.06 – 0.198) compared with longitudinal sections (0.032 pixels/um^2; CI95% 0.023 – 0.04; Wald Chi-square 7.58, p=0.006) in control donors. Similarly AQP4 positive pixels were higher in sagittal (0.23 pixels/um^2; CI95% 0.14 – 0.32) compared with longitudinal (0.073 pixels/um^2; CI95% 0.047 – 0.099; Wald Chi-square 13.78, p<0.001) sections. Similar findings were confirmed in donors with demyelinating CNS diseases.